IEEE Robotics and Automation Letters (RAL) paper presented at the
2020 IEEE/RSJ International Conference on Intelligent Robots and Systems (IROS)
October 25-29, 2020, Las Vegas, NV, USA (Virtual)

Elastomeric Continuously Variable Transmission Combined with Twisted String Actuator*

Seungyeon Kim[1], Jaehoon Sim[1], and Jaeheung Park[1,2]

***Abstract*— Electric motors, with a fixed reduction ratio, have a large unused operating region when mimicking muscle movements owing to the difference between the force-velocity curves of electric motors and muscles. This unused region can be reduced by changing the reduction ratio according to the external force. However, the conventional continuously variable transmissions (CVTs) are large and heavy. Elastomeric CVT (ElaCVT), a new concept relating to CVT, is designed in this study. The primary purpose of ElaCVT is to expand the operating region of a twisted string actuator (TSA) and duplicate the force-velocity curve of the muscles by passively changing the reduction ratio according to the external load applied to the end of the TSA. A combination of ElaCVT and TSA (ElaCVT-TSA) is proposed as a linear actuator that mimics the characteristics of muscles. The deformation of *elastomer* changes the reduction ratio without the need for complicated mechanisms. This enables the CVT to be small and lightweight so that it can be applied to various robotic systems. The performance of the ElaCVT-TSA was evaluated by means of the experiments, and the results show that the reduction ratio was passively and continuously adjusted as the external load changed. The ElaCVT has a cylindrical shape with a length of 27 mm, a diameter of 24 mm, and weighs 12 g. The reduction ratio in the maximum velocity mode is approximately 2.31 times the reduction ratio in the maximum torque mode.**

I. INTRODUCTION

The mimicking of human hand motion constitutes a vital research direction demanded by many modern robotic applications, which include humanoid robots that imitate human motion, prosthesis to replace human hands, and wearable devices that assist human hand movements. Until now, several devices have been developed using electric motors, and robotic hands that employ new types of actuators, like pneumatic actuators and shape memory alloy actuators, have been designed [1][2][3]. Various approaches, concerning robotic hands, have been investigated for improvement in terms of dexterity, force, weight, and volume [4][5].

However, to our knowledge, there exists no robotic hand that simultaneously realizes the weight, size, force, and dexterity of the human hand and continues to remain a challenge [5]. One of the several reasons why contemporary robotic hands cannot surpass the traits of human hands is the challenge associated with reducing the size of the actuators without losing power capacity [6]. Therefore, the properties of muscles, efficient muscle placement using tendon, and adaptable reduction ratios are required for a versatile end-effector with high degrees of freedom in small proportions like human hands [7][8][9].

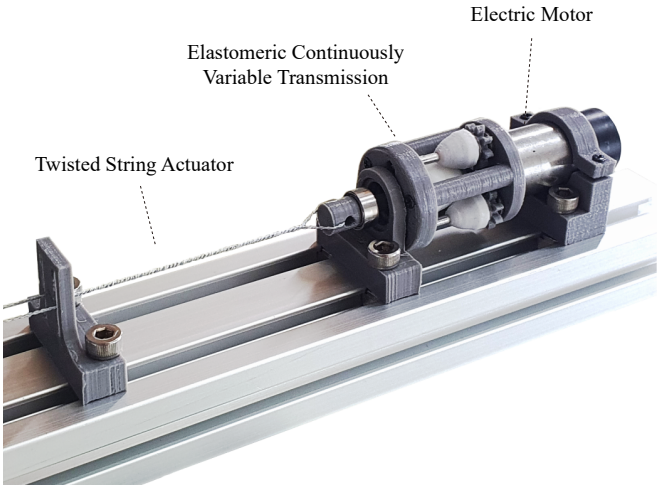

Fig. 1. ElaCVT-TSA: Combination of ElaCVT and TSA

The use of electric motors with a variety of mechanisms that convert the rotational force of a motor into linear forces is a commonly used method to achieve the characteristics of muscles. By converting rotational forces into linear forces and using strings as tendons, heavy and bulky actuators can be placed on the forearm. Schmitz et al. [10] placed tendon-driven actuators in the palm and forearm to maintain versatility in small robotic hands. Furthermore, Bridgwater et al. [11] designed a robotic hand using a tendon connected to an electric motor with a ball screw.

Twisted string actuator (TSA) is a method comprising electric motors and strings and is an actuator that employs the contraction force that occurs when multiple strings are twisted [12][13]. As the TSA converts rotational the force of a motor to linear force using a lightweight and straightforward structure, it has been applied to various robotic systems. Palli et al. [14] implemented a robotic hand and wrist with 22 degrees of freedom, using 24 TSAs in the forearm. However, a TSA with a high reduction ratio is not appropriate to be accelerated to the contraction velocities of muscles. To overcome the limitation of TSAs, TSAs with variable reduction ratio mechanisms have been studied by adjusting the reduction ratio by means of an external load, which is one of the properties of muscles.

*This work was supported by Industrial Strategic Technology Development Program (No. 20004953) funded By the Ministry of Trade, Industry & Energy(MOTIE, Korea)

[1]The authors are with DYROS Lab, Graduate School of Convergence Science and Technology, Seoul National University, Seoul, Republic of Korea. {ksy0711, simjeh, park73}@snu.ac.kr

[2]Jaeheung Park is also with Advanced Institutes of Convergence Technology(AICT), Suwon, Republic of Korea. He is the corresponding author of this paper.

Jeong and Kim [15] designed a 2-speed small transmission mechanism based on the TSA mechanism consisting of two motors. One motor provides the contraction force, while the other one is used to switch between the force mode and speed mode, by changing the twisted radius. Furthermore, they demonstrated the feasibility of a 2-speed dual-mode TSA by applying it to a robotic hand. However, the mode change process interrupted continuous motion. Singh et al. [16] proposed a passively adjustable TSA with springs placed between two strings that could maintain a small reduction ratio under a small external force. This passive adjustable TSA showed that continuous variable transmission (CVT) could be effectively used to cover the operating region of muscles. However, it remains as a limitation that the amount of reduction ratio variation decreases as the TSA contracts, because the change of reduction ratio depends on the amount of spring compression.

Various types of CVTs have been developed, and many commercial products already exist. However, these CVTs have a complex structure in order to transmit high torque without slip. Moreover, when changing the reduction ratio, these CVTs employ use hydraulic pumps to overcome reaction forces like friction. Although CVTs, which convert the reduction ratio passively, are used in relatively low power engines such as motorcycles, these CVTs use inertia forces, which are generated at high rotational speeds. Therefore, it is impossible to reduce the size and weight of existing CVTs for robotic applications.

To expand the operating region of TSAs and mimic the force-velocity curve (FV curve) of muscles, in this study, we designed a novel elastomeric CVT (ElaCVT), which can be applied to small-size robotic applications such as robotic hands (Fig. 1). The reduction ratio of the ElaCVT is passively changed by means of an external load on the TSA that compresses the elastomer. Additionally, by combining the ElaCVT and TSA (ElaCVT-TSA), we propose a new concept for the linear actuator module, which can be used as a muscle-like actuator. The twisted string mechanism amplifies the relatively small reduction ratio of the ElaCVT.

This paper has been presented as follows. In Section II, we compare the FV curves of muscles and electric motors and demonstrate the necessity of a CVT to mimic the force-velocity characteristics of muscles. In Section III, the structure of the proposed ElaCVT-TSA is described and the passively changing reduction ratio mechanism by means of an external force is explained. To demonstrate the performance of the ElaCVT-TSA, the experimental results of the contraction test, with various external loads, are shown in Section IV. Finally, the conclusions are presented in Section V.

II. COMPARISON OF OPERATING REGIONS

Various actuators have different operating characteristics. Comparing the operating region, using the *FV curve* of different actuators, is an essential step in selecting appropriate actuators.

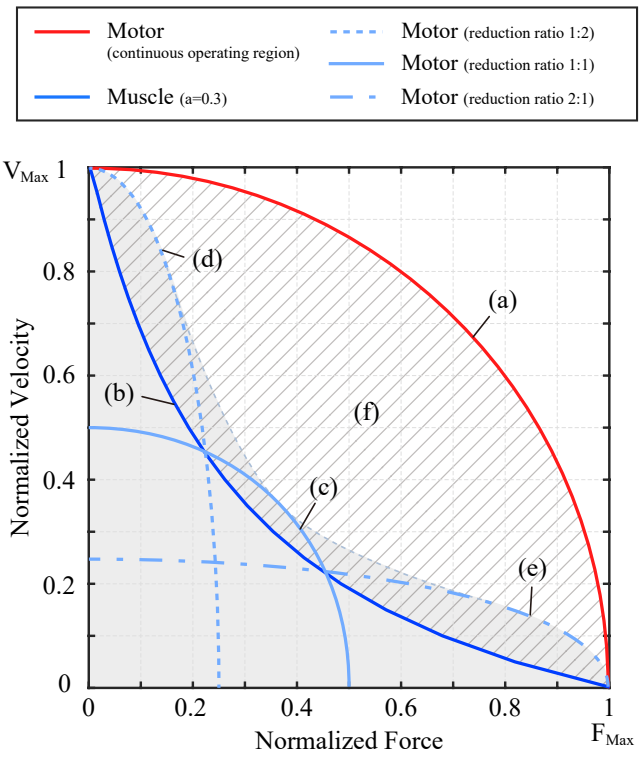

Fig. 2. (a) FV curve of an electric motor, (b) FV curve of muscle (a=0.3), (c), (d), (e) FV curves of an electric motor with CVT, (f) unused area when simulating muscle motion. The power capacity of (a) is four times that of (c).

TABLE I
COMPARISON BETWEEN TWO COMMERCIALLY AVAILABLE ELECTRIC MOTORS WITH DIFFERENT POWER CAPACITIES

Product Name	Maxon, EC-max 16	Maxon, EC-max 22
Power capacity	5 W	12 W
Nominal speed	5840 rpm	8040 rpm
Nominal torque	3.23 mNm	10.2 mNm
Diameter	16 mm	22 mm
Length	24 mm	32 mm
Weight	36 g	83 g

The continuous operating region of a general electric motor can be represented as a quadrant of the circle owing to the physical limitations of the materials used in motors, such as insulation damage of the wire that can be caused by high temperature. The mechanism that converts torque of the motor into linear force can be regarded as a reducer with a fixed reduction ratio; the FV curve of the linear actuator, using an electric motor, can be represented by the same quadrant as the operating region of the motor. The red line in Fig. 2(a) is the normalized FV curve of a linear actuator.

The FV curve of muscles can be approximated using the following hyperbolic equation [17].

$$(P + a)(v + b) = (P_0 + a)b = const. \quad (1)$$

The variables P, P_0, and v are the load, maximum isometric force, and contraction velocity of the muscle, respectively. The terms a and b are constant parameters obtained experimentally for each muscle. For mammalian skeletal muscles, a/P_0 approximately lies between 0.15 to 0.30 [18]. The normalized FV curve for muscles, whose maximum isometric force (P_0) and maximum contraction velocity are 1, with $a = 0.3$, is depicted in Fig. 2(b).

The operating regions of the muscle and electric motor have different shapes. The muscle has a concave shape, and the electric motor has a convex shape. The hatched area (Fig. 2(f)) between these two curves is unusable when mimicking the motion of muscles, but it occupies a large portion of the operating region of the motor. The muscle with the smaller parameter a result in an FV curve that has a more concave shape, and larger hatched area. However, the use of a motor with smaller power capacity cannot achieve the maximum speed or force of the muscle, and it is, therefore, impossible to reduce this area without the use of additional mechanisms.

Fig. 2(c), (d), and (e) show the FV curves of the motor with a CVT, whose change in reduction ratio is 2:1, 1:1, and 1:2. The grey area below these graphs represents the operating region of the motor with the CVT, and effectively covers the operating region of the muscles. In this case, the required power capacity of the motor with CVT is four times smaller than the power capacity of the motor without CVT. In Table I, a compression of the specifications of two commercially available motors with different power capacities is shown. The first is EC-max 16, 5 W motor, which is used in this study. The second one is EC-max 22, which has a 12 W power capacity. The EC-max 16 weighs less than half the EC-max 22, and this shows that there is a significant weight difference, depending on the power capacity of the motors. In robotic hands that employ multiple actuators, the weight of the entire system can be significantly reduced, if the ElaCVT-TSA is designed lighter than an actuator with a large unused region.

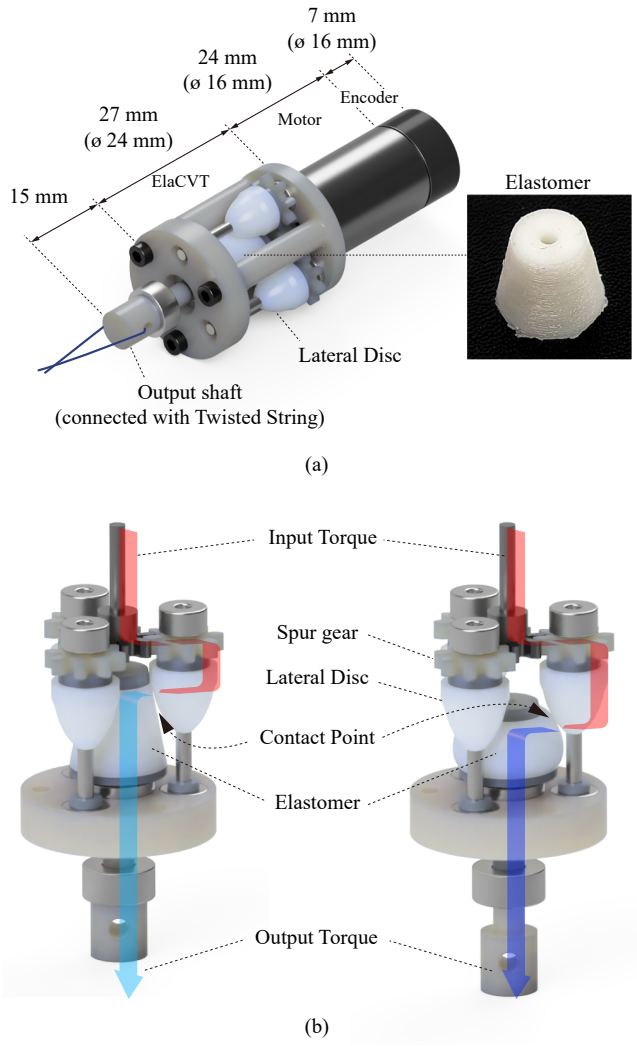

Fig. 3. Configuration of the ElaCVT-TSA, (a) Dimension of the ElaCVT-TSA, (b) Inner structure of the ElaCVT without the outer case. The left image depicts the maximum velocity mode, while the right image depicts the maximum torque mode.

III. DESIGN OF THE ELASTOMERIC CONTINUOUS VARIABLE TRANSMISSION

In this section, we introduce the actuator module that combines the ElaCVT and TSA. Furthermore, we explain the structure and mechanism of the newly proposed ElaCVT, including the advantages of the ElaCVT.

A. Structure of ElaCVT

In Fig. 3(a), an ElaCVT-TSA is depicted, and the inner structure of the ElaCVT is illustrated in Fig. 3(b). The ElaCVT consists of a rigid lateral disc and elastomer, which is directly connected to the output shaft. The input torque from the motor is transmitted to the lateral disc by means of spur gears to the output shaft using friction between the lateral disc and elastomer. The mechanisms that convert the rotational force to linear force can be applied to the end of the ElaCVT. The ball screw and lead screw are commonly used mechanisms. However, in this study, we employ the TSA. Although ball screw mechanisms have better efficiency and are more reliable than the TSA, they not only are heavier than the TSA but also require an additional mechanism to enable axial movement. On the other hand, the flexibility of strings used to the TSAs facilitates axial movement without the need for additional mechanisms, which reduces the weight of the overall system. The output shaft of the ElaCVT is connected to the TSA, and the torque is converted into a linear force. With this structure, the external load applied to the end of the TSA can directly compress the elastomer the along axial direction, and change the reduction ratio continuously (Fig. 3(b)).

Since the maximum static friction between the elastomer and each lateral disc is equal, the higher the number of lateral discs used, the larger the torque that can be transmitted without slip. In this study, three lateral discs were used, considering the size of elements such as bearings. All the parts were manufactured using a 3D printer, except the bearings and rotating shafts. The ElaCVT has a cylindrical

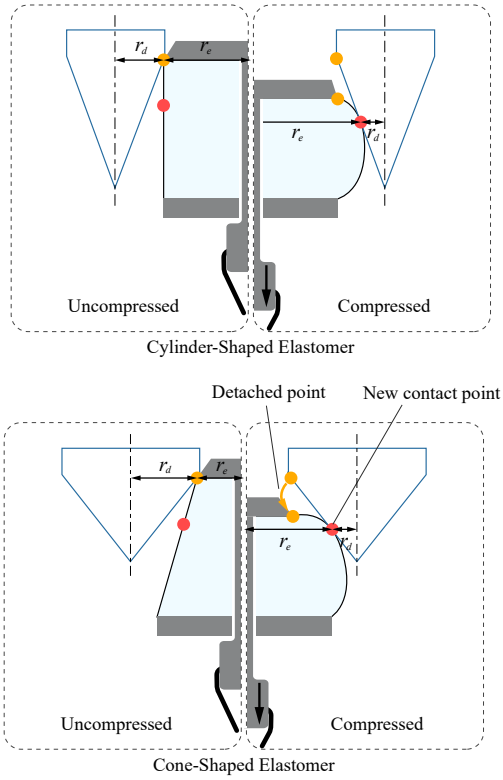

Fig. 4. Different lateral disc shapes depending on the shapes of the elastomer. The orange points are the contact points when the elastomer is uncompressed, and red points are newly attached contact points after compression. Using a cone-shaped elastomer, the amount of contact radius change increases.

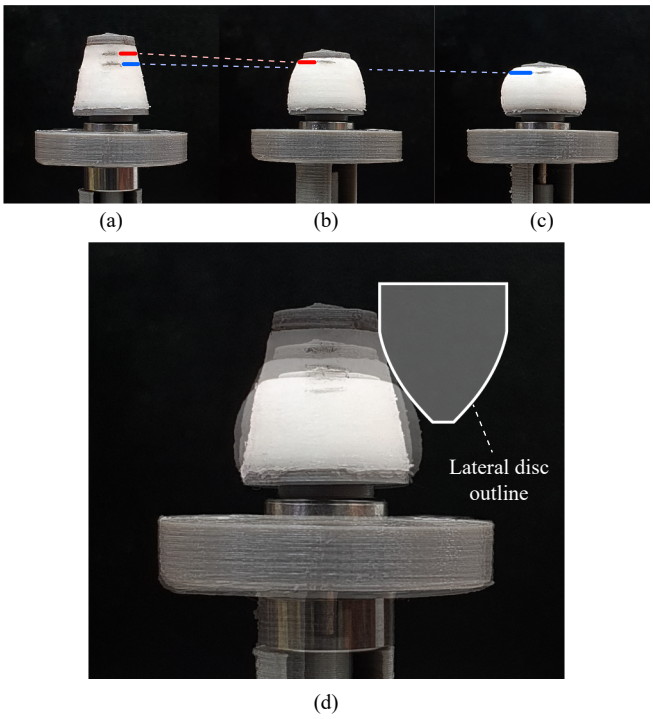

Fig. 5. Deformation of elastomer according to the amount of compression, (a) 0 mm, (b) 2 mm, (c) 4 mm, red and blue line indicates the same location on the elastomer, respectively. (d) Overlapped images with the outline of the lateral disc.

shape with a length of 27 mm, a diameter of 24 mm (Fig. 3(a)), and weighs 12 g.

B. Design of Elastomer and Lateral Disc

The elastomer is a crucial part that allows the change of the reduction ratio, and the material and shape of the elastomer directly affect the performance of the ElaCVT. Various shapes of elastomer were tested, using silicone of multiple stiffnesses. The stiffness of the elastomer should be selected considering the output torque of the motor. If a low torque motor with a high stiffness elastomer is used, the motor reaches the torque limit before the reduction ratio changes. Conversely, if a high torque motor with a low stiffness elastomer is used, a large part of the operating region of the motor is used, only at a high reduction ratio. We used a silicone with 12 Shore A, and the lateral discs were covered with a thin layer of the same silicone to prevent wear of the lateral discs and elastomer.

We shaped the elastomer into a cone to increase the change in the reduction ratio. Simplified shapes of the lateral discs, depending on the cylinder-shaped and cone-shaped elastomers are illustrated in Fig. 4. When the elastomer is compressed, it forms new contact points by filling the gaps between the lateral discs and the elastomer. In Fig. 4, r_e and r_d are the radii from the rotational axis of the elastomer and the lateral disc to the contact point. The ratio of these radii, $r_e : r_d$, represents the reduction ratio of the ElaCVT. As the elastomer is compressed, r_e becomes larger, and r_d decreases, the transmitted torque is amplified, and the angular velocity decreases. The use of a cone-shaped elastomer can increase the radial change of the lateral disc and elastomer disc. Therefore, a larger reduction ratio change is implemented.

Elastomers applied to the ElaCVT have a lower diameter of 12 mm, an upper diameter of 8 mm, and a height of 10 mm with a weight of 1 g. The size of the elastomer was selected, considering the size and output of the motor used (Maxon, EC-max 16). To determine the outer line of the lateral disc corresponding to the elastomer, we conducted deformation experiments. Deformed elastomers and the outline of the lateral disc are depicted in Fig. 5. We then interpolated the outermost points to complete the outline of the lateral discs. To prevent the disconnection between the elastomer and lateral discs due to manufacturing errors, we employed a 5% enlarged outline to produce the lateral disc.

The size of the ElaCVT can be reduced by using a small elastomer. However, given that transmittable torque is also reduced when using a smaller elastomer, the appropriate size of the elastomer should be considered.

C. Advantages of ElaCVT

The ElaCVT, which implements the reduction ratio change by using the shape deformation of the elastic body, has advantages that are suitable for the robotics field.

First, in the reduction ratio change process, the previous

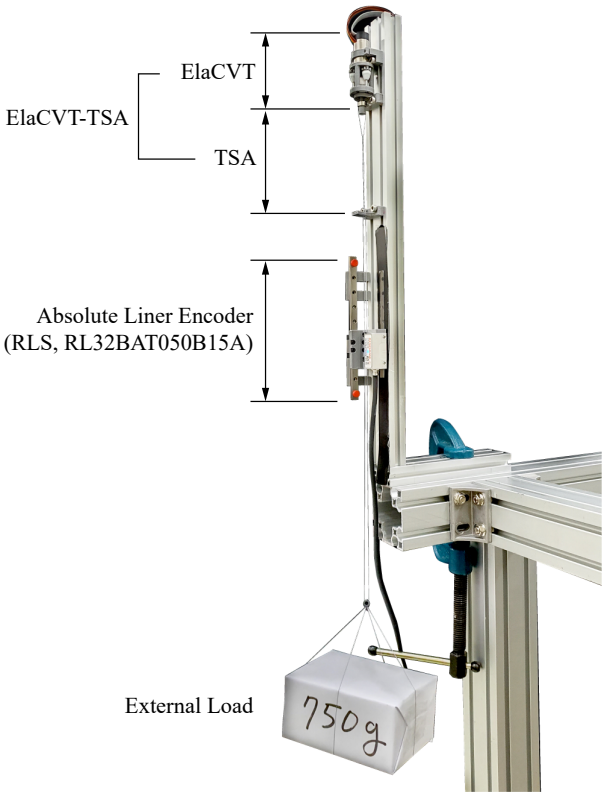

Fig. 6. Experimental setup to evaluate ElaCVT-TSA

contact point detaches and does not slip to move to the new contact point, and a new contact point is generated through the deformation of the elastic body. This process reduces friction resistance. The differently located contact points as the elastomer is compressed are shown in Fig. 5.

Second, due to the above advantage, the structure of the ElaCVT can be simplified, given that the load on the output shaft is sufficient to compress the elastomer, unlike conventional CVTs that require a linear actuator.

Third, when combined with a reducer that converts rotational force to linear force, the reduction ratio is changed passively by the linear force, applied to the end, without any additional mechanism. Thus, the combination of TSA and ElaCVT facilitates the actuator module, which simulates muscle characteristics, through the light and straightforward structure.

Additionally, due to the internal structure of the ElaCVT, the motor shaft is decoupled from the output shaft along the axial direction. Any additional structures, such as thrust bearings, are not required to prevent damage to the motor from high axial loads or impacts at the output shaft.

IV. PERFORMANCE EVALUATION

To evaluate the performance of the newly proposed ElaCVT-TSA, an experimental setup was designed. In this chapter, we introduce the experimental setup, and evaluate the reduction ratio change capability of the ElaCVT through the contractions under different external loads.

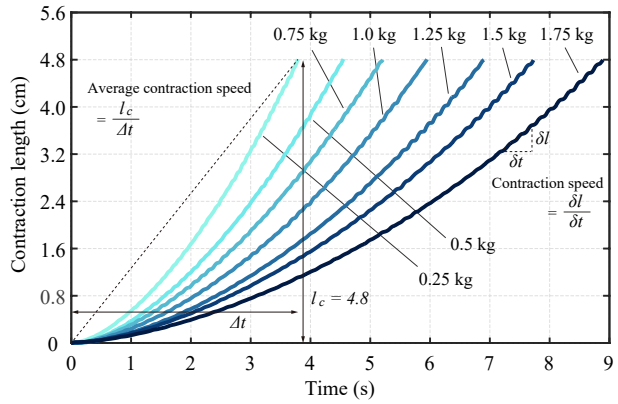

Fig. 7. Contraction length with different external loads under constant motor speed, 2000 rpm. With constant motor speed, the contraction speed decreases as contraction length increases due to TSA. Average contraction speed was used to exclude the effect of TSA when evaluated the reduction ratio change of ElaCVT.

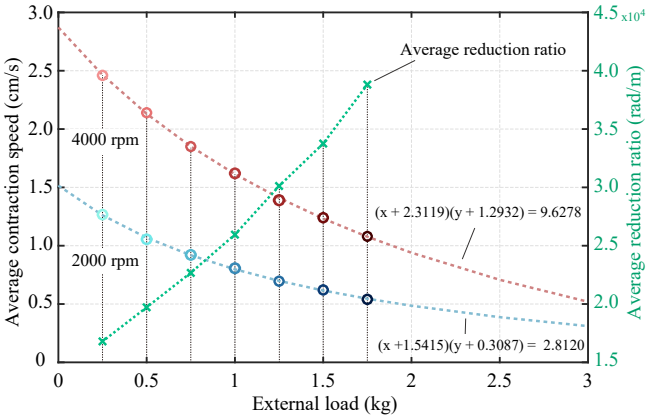

Fig. 8. FV curves of the ElaCVT-TSA under different motor speeds, 2000 rpm, and 4000 rpm. Circle points represent experimental data. The green dash line shows the average reduction ratio of the ElaCVT-TSA under different external loads.

A. Experimental Setup

In Fig. 6, the experimental setup used to evaluate the performance of the ElaCVT-TSA is illustrated. The string used for the TSA was the Dyneema fishing line, whose diameter was 0.5 mm. Without external load, the distance from the string hole on output shaft to string slit was 10 cm. At the end of the TSA, an absolute linear encoder (RLS, RL32BAT050B15A) was installed to measure the contraction length. To reduce the influence of string elongation on the experimental results, we repeated the contraction 50 times with an external load of 1.75 kg before the experiments.

B. Contraction with Fixed external load

To evaluate the primary purpose of the proposed ElaCVT-TSA, simulating a muscle-like FV curve, we measured the contraction length under different external loads, which ranged from 0.25 kg to 1.75 kg. In all experiments, the motor was controlled at a constant speed. Fig. 7 shows the results of the contraction length from 0 cm (untwisted) to 4.8 cm,

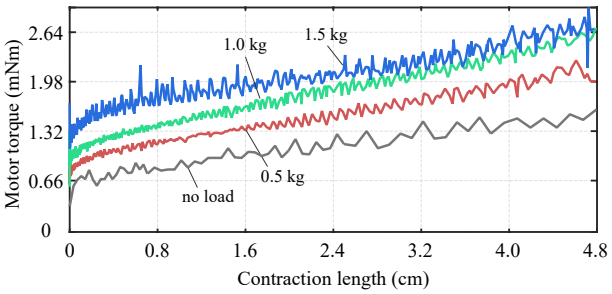

Fig. 9. Motor torque with the different external loads, 0.5 kg , 1.0 kg, and 1.5 kg. The motor torque increased because the reduction ratio of TSA decreases as TSA contracts.

maintaining a motor speed of 2000 rpm. As the external force increased, the time taken to reach the target point increased, which implies that the external force deformed the elastomer of the ElaCVT. Moreover, the reduction ratio was converted to a high reduction ratio. However, the results show that the contraction speed of the ElaCVT-TSA with a constant motor speed increased as the contraction length increased, because the reduction ratio of the TSA decreased. To exclude the effect of the TSA on the reduction ratio, the average contraction speed was used to construct the FV curves and to calculate the average reduction ratio in Fig. 8.

The FV curves of the ElaCVT-TSA are shown in Fig. 8. The same experiments were repeated using a motor speed of 4000 rpm, and the results are shown together. As the motor speed doubled, the average contraction speed doubled in all cases, which implies that the ElaCVT is only affected by the magnitude of the external force, and not the speed and torque of the motor. The experimental data are fitted with a hyperbolic function, which represents the FV curve of muscles, and the functions are plotted as dotted lines in Fig. 8. Each calculated hyperbolic function shows that the experimental results simulated the FV curve of the muscle.

The green dash line in Fig. 8 shows the average reduction ratio which was changed under the different external loads. The average reduction ratio at 1.75 kg was averagely 2.31 times the average reduction ratio at 0.25 kg (from 16776 rad/m to 38811 rad/m).

The input torque of the TSA is proportional to the output force at the same contraction length [12]. Fig. 9 shows the motor torque according to the contraction length under 0.5 kg, 1.0 kg, and 1.5 kg external loads, and the experiments were conducted at a motor speed of 2000 rpm. By subtracting the no-load torque, the average motor torques required for the contractions for each experiment are found to be 0.46 mNm, 0.74 mNm, and 1.02 mNm. Using the average motor torques, the efficiency of ElaCVT can be calculated as $\eta = P_{out}/P_{in}$ where P_{in} is the input power, which is the product of motor torque and angular velocity, and P_{out}, which is the product of external load and average contraction speed. The efficiencies under 0.5 kg, 1.0 kg, and 1.5 kg external loads at 2000 rpm are 56%, 52% and 44%, respectively.

The reduction ratio at 1.5 kg increased to 1.70 times the reduction ratio at 0.5 kg (from 19853 rad/m to 33727 rad/m).

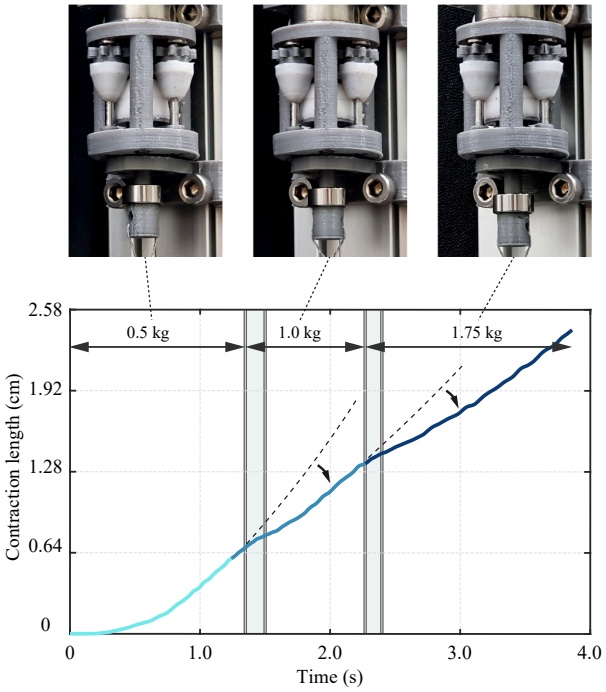

Fig. 10. Contraction length with gradually increased external load

The motor torque should have increased 1.76 times with the tripled external load, given that the 1.70 times increased reduction ratio. However, the average motor torque of the ElaCVT-TSA increased to about 2.22 times (from 0.46 mNm to 1.02 mNm). This difference was partly attributed to the friction between the elastomer and lateral discs. Ideally, the contact points between the elastomer and the lateral discs should be point contacts. However, the lateral discs were scaled up to ensure sufficient friction. This created an area where slip occurred, resulting frictional losses.

C. Contraction with Variable external load

The advantage of the ElaCVT-TSA is that the reduction ratio is passively adjusted depending on the external load regardless of the operation of the motor. This does not generate any discontinuities in the process while changing the reduction ratio. To evaluate this property, we conducted an experiment where the external load increased gradually as the ElaCVT-TSA contracted. The motor was controlled at a constant speed of 2000 rpm.

In Fig. 10, the contraction length of the ElaCVT-TSA over time and shape of the elastomer at each external load are shown. The reduction ratio of the ElaCVT changed smoothly as the load increased to 0.5 kg, 1.0 kg, and 1.75 kg. Moreover, we observed that the elastomer was compressed gradually. The result consists of multiple pieces of the results of the fixed external load shown in the previous section. As shown in Fig. 7, the contraction speed increased as the TSA contracted under the constant motor speed. However, the contraction speed decreased in grey regions, shown in Fig. 10, because the reduction ratio increased by means of the passively deformed elastomer.

TABLE II
THE SPECIFICATIONS OF ELACVT-TSA AND EACH COMPONENT

Component Name	Motor with encoder Maxon, EC-max 16	ElaCVT	TSA	ElaCVT-TSA
Diameter	16mm	24 mm	1 mm (2 × 0.5 mm)	24 (maximum value)
Length	31 mm	27 mm	115 mm (including a string connector)	173 mm (58 mm without strings)
Weight	39 g	12 g	$<$ 1 g	52 g
Power capacity	5 W	-	-	5 W
Nominal speed	5840 rpm	-	-	-
Nominal torque	3.23 mNm	-	-	-
Reduction ratio	1 : 1	1 : 1∼2.31 : 1	16776 : 1 *	16776 : 1 ∼ 38811 : 1 *
Maximum continuous contraction Speed	-	-	-	0.037 m/s **
Maximum continuous contraction Force	-	-	-	(20 N) ***

* Reduction ratio of TSA represents [Input rotational speed (rad/s) : Output linear contraction speed (m/s)]. The reduction ratio of TSA is average value along contraction length from 0 cm to 4.8 cm.

** Maximum continuous contraction Speed is calculated as multiplying the reduction ratio and nominal speed of the motor.

*** The hardware broke down before reached the Maximum continuous contraction Force. The value is the maximum external load we tested.

D. Specifications and Limitations of ElaCVT-TSA

The specifications of the ElaCVT-TSA manufactured in this study, and other elements are summarized in Table II. This includes the string and connector of length 115 mm, and the total length of the ElaCVT-TSA recorded as 173 mm. Furthermore, the total weight of the ElaCVT-TSA is 52g. The reduction ratio of the TSA was expressed as the ratio of the input rotational speed and the output shrinkage speed, and, the average reduction ratio was calculated using the average speed during the contraction to 4.8 cm. The final reduction ratio from the motor speed to the contraction speed of the ElaCVT-TSA was passively and continuously varied from 16776:1 to 38811:1 according to external forces, and the maximum contraction force could not be measured due to the breakdown of the connector between the elastomer and output shaft.

We fabricated and verified the ElaCVT-TSA using a fused deposition modeling 3D printer using a PLA filament. However, some limitations should be improved to apply this concept to a wide range of areas. The first is the use of more rigid materials like aluminum, using which small and strong structures can be designed. In this study, we were unable to evaluate the maximum contraction force of the ElaCVT-TSA, because it broke down before reaching the maximum contraction force. Furthermore, the relatively large size of the ElaCVT devaluates the advantage of using small motors.

Second, the current design of the ElaCVT does not enable to utilize the maximum specifications of the motor. The maximum no-load speed of the motor, EC-max16, used in this study was 13500 rpm, but the maximum input speed of ElaCVT was about 9090 rpm. Moreover, the ElaCVT has lower efficiency compared to commercially available gearboxes. Thus, the efficiency of the ElaCVT was about 50%. Some losses were caused by a poor precision structure including 3D printed spur gears and friction generated by the TSA.

Third, as described in Section II, it is necessary to change the reduction ratio by 4 times to cover the operating region of the muscle efficiently. However, this study was only able to reach 2.31 times. Additionally, slippage was observed between the elastomer and the lateral disc when more than 3.3 mNm torque was applied. We also applied a belt dressing between the elastomer and the lateral disc to increase friction, but this does not constitute a fundamental solution. In this study, silicon was used to test the elastomers of different stiffnesses. However, silicon, as a material, does not have high friction characteristics. Therefore, further studies concerning the material and shape of the elastomer are needed to increase the amount of reduction ratio change and maximum transmittable torque.

V. CONCLUSION AND FUTURE WORK

In this paper, we presented the ElaCVT, which is a novel CVT using an elastomer to implement the change of reduction ratio, and proposed a new concept of a linear actuator, ElaCVT-TSA, which combines the proposed ElaCVT and a TSA. Unlike conventional CVTs, which are large and heavy, ElaCVT can be manufactured to be small and light and can be applied to small-size robotic applications such as robotic hands.

ElaCVT-TSA passively and continuously changes the reduction ratio depending on the external load applied at the end of the TSA and expands the operating region of the TSA. It was also found that the operating region of the ElaCVT-TSA could mimic the FV curves of muscles through experiments with various external loads. The ElaCVT has a cylindrical shape of 27 mm in length, 24 mm in diameter, and weighs 12 g. The reduction ratio in the maximum velocity mode was 2.31 times that in the maximum torque mode.

We hope to develop a new, fully actuated robotic hand using multiple ElaCVT-TSAs. Based on this study, we plan

to improve the efficiency of the ElaCVT and increase the reduction ratio variation by optimizing the shape and material of the elastomer. Additionally, the size of the ElaCVT-TSA will be reduced to realize a human hand-sized robotic hand.

REFERENCES

[1] K. Andrianesis and A. Tzes, "Development and control of a multifunctional prosthetic hand with shape memory alloy actuators," *Journal of Intelligent & Robotic Systems*, vol. 78, no. 2, pp. 257–289, 2015.

[2] A. A. M. Faudzi, J. Ooga, T. Goto, M. Takeichi, and K. Suzumori, "Index finger of a human-like robotic hand using thin soft muscles," *IEEE Robotics and Automation Letters*, vol. 3, no. 1, pp. 92–99, 2017.

[3] V. Wall, G. Zöller, and O. Brock, "A method for sensorizing soft actuators and its application to the rbo hand 2," in *2017 IEEE International Conference on Robotics and Automation (ICRA)*. IEEE, 2017, pp. 4965–4970.

[4] J. Hughes, U. Culha, F. Giardina, F. Guenther, A. Rosendo, and F. Iida, "Soft manipulators and grippers: a review," *Frontiers in Robotics and AI*, vol. 3, p. 69, 2016.

[5] C. Piazza, G. Grioli, M. Catalano, and A. Bicchi, "A century of robotic hands," *Annual Review of Control, Robotics, and Autonomous Systems*, vol. 2, pp. 1–32, 2019.

[6] J. Zhang, J. Sheng, C. T. ONeill, C. J. Walsh, R. J. Wood, J.-H. Ryu, J. P. Desai, and M. C. Yip, "Robotic artificial muscles: Current progress and future perspectives," *IEEE Transactions on Robotics*, vol. 35, no. 3, pp. 761–781, 2019.

[7] J. D. Madden, N. A. Vandesteeg, P. A. Anquetil, P. G. Madden, A. Takshi, R. Z. Pytel, S. R. Lafontaine, P. A. Wieringa, and I. W. Hunter, "Artificial muscle technology: physical principles and naval prospects," *IEEE Journal of oceanic engineering*, vol. 29, no. 3, pp. 706–728, 2004.

[8] R. J. Schwarz and C. Taylor, "The anatomy and mechanics of the human hand," *Artificial limbs*, vol. 2, no. 2, pp. 22–35, 1955.

[9] E. Azizi, E. L. Brainerd, and T. J. Roberts, "Variable gearing in pennate muscles," *Proceedings of the National Academy of Sciences*, vol. 105, no. 5, pp. 1745–1750, 2008.

[10] A. Schmitz, U. Pattacini, F. Nori, L. Natale, G. Metta, and G. Sandini, "Design, realization and sensorization of the dexterous icub hand," in *2010 10th IEEE-RAS International Conference on Humanoid Robots*. IEEE, 2010, pp. 186–191.

[11] L. B. Bridgwater, C. Ihrke, M. A. Diftler, M. E. Abdallah, N. A. Radford, J. Rogers, S. Yayathi, R. S. Askew, and D. M. Linn, "The robonaut 2 hand-designed to do work with tools," in *2012 IEEE International Conference on Robotics and Automation*. IEEE, 2012, pp. 3425–3430.

[12] G. Palli, C. Natale, C. May, C. Melchiorri, and T. Wurtz, "Modeling and control of the twisted string actuation system," *IEEE/ASME Transactions on Mechatronics*, vol. 18, no. 2, pp. 664–673, 2012.

[13] I. Gaponov, D. Popov, and J.-H. Ryu, "Twisted string actuation systems: A study of the mathematical model and a comparison of twisted strings," *IEEE/ASME Transactions on Mechatronics*, vol. 19, no. 4, pp. 1331–1342, 2013.

[14] G. Palli, C. Melchiorri, G. Vassura, U. Scarcia, L. Moriello, G. Berselli, A. Cavallo, G. De Maria, C. Natale, S. Pirozzi, *et al.*, "The dexmart hand: Mechatronic design and experimental evaluation of synergy-based control for human-like grasping," *The International Journal of Robotics Research*, vol. 33, no. 5, pp. 799–824, 2014.

[15] S. H. Jeong and K.-S. Kim, "A 2-speed small transmission mechanism based on twisted string actuation and a dog clutch," *IEEE Robotics and Automation Letters*, vol. 3, no. 3, pp. 1338–1345, 2018.

[16] H. Singh, D. Popov, I. Gaponov, and J.-H. Ryu, "Twisted string-based passively variable transmission: Concept, model, and evaluation," *Mechanism and Machine Theory*, vol. 100, pp. 205–221, 2016.

[17] A. V. Hill, "The heat of shortening and the dynamic constants of muscle," *Proceedings of the Royal Society of London. Series B-Biological Sciences*, vol. 126, no. 843, pp. 136–195, 1938.

[18] R. Close, "Dynamic properties of mammalian skeletal muscles." *Physiological reviews*, vol. 52, no. 1, pp. 129–197, 1972.